Cell

DNA Sequence-Dependent Compartmentalization and Silencing of Chromatin at the Nuclear Lamina

Joseph M. Zullo,[1,8] Ignacio A. Demarco,[3,8] Roger Piqué-Regi,[2,4] Daniel J. Gaffney,[2,4] Charles B. Epstein,[5,6] Chauncey J. Spooner,[3] Teresa R. Luperchio,[7] Bradley E. Bernstein,[5,6] Jonathan K. Pritchard,[2,4] Karen L. Reddy,[7] and Harinder Singh[1,3,*]

[1]Department of Molecular Genetics and Cell Biology
[2]Department of Human Genetics
The University of Chicago, Chicago, IL 60637, USA
[3]Department of Discovery Immunology, Genentech, South San Francisco, CA 94080, USA
[4]Howard Hughes Medical Institute, 929 East 57th Street, Chicago, IL 60637, USA
[5]The Broad Institute of Harvard and Massachusetts Institute of Technology, Cambridge, MA 02142, USA
[6]Department of Pathology, Massachusetts General Hospital and Harvard Medical School, Boston, MA 02114, USA
[7]Department of Biological Chemistry, Center for Epigenetics, The Johns Hopkins University School of Medicine, Baltimore, MD 21205, USA
[8]These authors contributed equally to this work
*Correspondence: harindsi@gene.com
DOI 10.1016/j.cell.2012.04.035

SUMMARY

A large fraction of the mammalian genome is organized into inactive chromosomal domains along the nuclear lamina. The mechanism by which these lamina associated domains (LADs) are established remains to be elucidated. Using genomic repositioning assays, we show that LADs, spanning the developmentally regulated *IgH* and *Cyp3a* loci contain discrete DNA regions that associate chromatin with the nuclear lamina and repress gene activity in fibroblasts. Lamina interaction is established during mitosis and likely involves the localized recruitment of Lamin B during late anaphase. Fine-scale mapping of LADs reveals numerous lamina-associating sequences (LASs), which are enriched for a GAGA motif. This repeated motif directs lamina association and is bound by the transcriptional repressor cKrox, in a complex with HDAC3 and Lap2β. Knockdown of cKrox or HDAC3 results in dissociation of LASs/LADs from the nuclear lamina. These results reveal a mechanism that couples nuclear compartmentalization of chromatin domains with the control of gene activity.

INTRODUCTION

The spatial localization of chromatin within the mammalian nucleus has been shown to be important for diverse genomic processes such as transcription (Sutherland and Bickmore, 2009), RNA processing (Lamond and Spector, 2003) as well as DNA repair and recombination (Misteli and Soutoglou, 2009). The inner nuclear membrane along with the nuclear lamina (INM-lamina) represent a prominent compartment within the nucleus, composed of a unique set of trans-membrane proteins (e.g., Emerin, Lap2β, and Lamin B receptor) and an underlying network of lamin intermediate filaments (Schirmer and Foisner, 2007). The INM-lamina makes extensive contacts with chromatin, and mutations of INM proteins have been implicated in a variety of human diseases.

Previously, we have demonstrated that the murine immunoglobulin heavy-chain (*IgH*) locus is positioned at the INM-lamina in nuclei of fibroblasts and hematopoietic progenitors, but is relocalized to the nucleoplasm in B-lineage progenitors concomitant with its activation for transcription and DNA recombination (Kosak et al., 2002; Reddy et al., 2008). Similarly, the *β-globin* and *CFTR* loci have also been shown to move away from the lamina during their developmental activation (Ragoczy et al., 2006; Zink et al., 2004). Finally, during *Caenorhabditis elegans* embryogenesis, developmentally regulated transgenes have been shown to associate with the nuclear lamina and to be released from this compartment in lineages in which they are activated (Meister et al., 2010).

While the above studies have relied upon three-dimensional imaging to examine nuclear dynamics of individual genes, DamID coupled with tiling array analysis has emerged as a powerful tool to systematically map interactions between chromatin and the INM-lamina on a genome-wide scale. This approach has utilized protein fusions between Lamin B (LMNB) or Emerin, and the *Escherichia coli* DNA adenine methyltransferase (Dam) to direct adenine methylation of DNA sequences that are in molecular proximity to the INM-lamina (Vogel et al., 2007). In human lung fibroblasts, this approach has revealed that one third of the genome is incorporated into large (100 kb to 10 Mb), sharply demarcated chromosomal regions termed lamina-associated domains (LADs) which are predominantly transcriptionally inactive (Guelen et al., 2008). In differentiating ES cells, many LADs have been shown to undergo

developmentally regulated assembly and disassembly (Peric-Hupkes et al., 2010). Collectively, the 3D-ImmunoFISH and DamID studies suggest a key function for the INM-lamina compartment in transcriptional silencing of large segments of the genome, including regions encoding developmentally regulated genes.

To test whether the activity of mammalian genes can be repressed by their interaction with the INM-lamina, we and others have used LacI-INM protein fusions to recruit test genes and genomic loci bearing *lacO* repeats to this compartment (Finlan et al., 2008; Kumaran and Spector, 2008; Reddy et al., 2008). Such inducible tethering to the INM-lamina can result in transcriptional repression of both the test gene and endogenous genes. Interestingly, tethering of a test gene to the INM-lamina requires passage through mitosis (Kumaran and Spector, 2008; Reddy et al., 2008), during which the nuclear envelope is broken down and reassembled (Webster et al., 2009). As chromatin and INM-lamina components are spatially constrained in the interphase nucleus, these observations suggest a plausible means of establishing such interactions in the context of nuclear envelope reassembly during mitosis. However, it remains to be determined if LAD interaction with the nuclear lamina is regulated by the cell cycle.

In principle, association of chromosomal domains with the INM-lamina could be DNA sequence and/or chromatin structure directed. Alternatively, it may reflect an intrinsic property of transcriptionally inactive chromatin which is not engaged with nucleoplasmic RNA Pol II factories (Zink et al., 2004). Finally, cumulative entropic effects of nonspecific DNA-protein interactions may account for peripheral positioning of certain chromatin domains, as has been proposed for the chromocenters in *Arabidopsis thaliana* (de Nooijer et al., 2009). To distinguish among these possibilities, we sought to determine if LADs contain DNA regions that are capable of positioning chromatin domains at the INM-lamina.

By characterizing the *IgH* and other LADs in murine fibroblasts and using genomic repositioning assays, we delineate DNA regions that direct the association of chromatin domains with the INM-lamina as well as transcriptional silencing. Association of such regions with the lamina requires mitosis and is likely initiated by localized recruitment of LMNB during late anaphase. Through fine mapping, we reveal numerous dispersed DNA sequences within LADs that are sufficient to direct the association of chromatin with the nuclear lamina. These are termed lamina-associating sequences (LASs) and are enriched for an extended GAGA motif that is bound by the vertebrate ortholog of the *Drosophila* GAGA factor, cKrox in a complex with HDAC3 and Lap2β. Knockdown of cKrox or HDAC3 reduces association of LASs as well as endogenous loci with the lamina and results in transcriptional de-repression. Our results reveal a molecular mechanism for coupling the compartmentalization of chromatin domains at the INM-lamina with the control of gene activity.

RESULTS

Delineation of the *IgH* and *Cyp3a* LADs

The murine *IgH* locus spans 3 Mb of DNA on chromosome 12 and is comprised of variable (V), diversity (D), joining (J) and constant (C) region segments. Given its large size and complex structure consisting of repeated gene segments we sought to analyze *IgH* DNA regions that are in molecular proximity to the INM-nuclear lamina in murine fibroblasts (Reddy et al., 2008). To this end, we performed DamID with a Dam-LMNB fusion protein in NIH 3T3 cells using high-density Affymetrix tiling arrays covering chromosomes 12 as well as 5 and 15. This experimental design enabled a comparison of the LAD(s) at the *IgH* locus with those in other chromosomal regions. Examination of the distal region of chromosome 12 revealed that the *IgH* locus comprised a single, continuous LAD (Figure 1A). Strikingly, the 5′ and 3′ ends of the *IgH* locus corresponded almost precisely to the boundaries of this LAD. This coincidence between the structural and functional boundaries of a multi-gene locus was also observed on chromosome 5 for a cluster of *Cyp3a* genes (Figure 1B), that encodes members of the cytochrome P450 superfamily. As is the case for the *IgH* locus, the *Cyp3a* genes are inactive in NIH 3T3 fibroblasts, and 3D-ImmunoFISH confirmed that they, like the *IgH* alleles, were positioned at the nuclear lamina (Figures 1A, 1B, and 1D). These genes undergo transcriptional activation in hepatocytes (Li et al., 2009) and as with the active *IgH* locus in pro-B cells we found them to be positioned in the nucleoplasm of FL83B hepatocytes (Figures 1E and 1F).

Using a modified version of the genome alteration detection analysis (GADA) algorithm (Pique-Regi et al., 2008), which delineates large, continuous regions of contrasting signal intensities, we identified 222 LADs in chromosomes 12, 5 and 15 (Figure S1A available online). The LADs ranged in size from 100 kb to 10 Mb and covered almost 40% of the three chromosomes. ChIPseq analyses of H3K4me3, H3K36me3 and CTCF were used to characterize the chromatin structure within LADs and their bordering regions (Figure S1B). Consistent with earlier results (Guelen et al., 2008), LADs displayed very low levels of transcription (Figure S1C) and reduced H3K36me3. Additionally, H3K4me3 and CTCF binding were substantially increased at LAD borders. Notably, a subset of boundaries displayed enrichment of H3K4me3 in the absence of CTCF binding suggesting that active promoters may function independently of CTCF to demarcate LADs. Murine LADs also exhibited a low GC content and were enriched for LTRs and LINEs (Figure S1D). While it has been suggested that LMNB and Lamin A (LMNA) segregate into discrete microdomains with differing associated chromatin states (Shimi et al., 2008) we found no substantial differences in the methylation patterns when DamID was performed using LMNB versus LMNA (data not shown).

LAD-Derived DNA Targets Chromatin to the Lamina

We undertook a functional analysis of LAD-derived DNA regions using two types of genomic repositioning assays. Initially, we employed a tagged chromosomal insertion site (TCIS) system based on site-specific recombination (Feng et al., 1999). This approach utilized a construct containing a thymidine kinase-hygromycin gene cassette flanked by heterospecific and inverted *loxP* sites and a *lacO* repeat segment (Figure 2A). We derived a clonal line bearing a single insertion of this construct that was positioned away from the nuclear lamina (Figure 2A, top panel). Test DNA sequences could be introduced at this insertion site using Cre/loxP mediated recombination and then

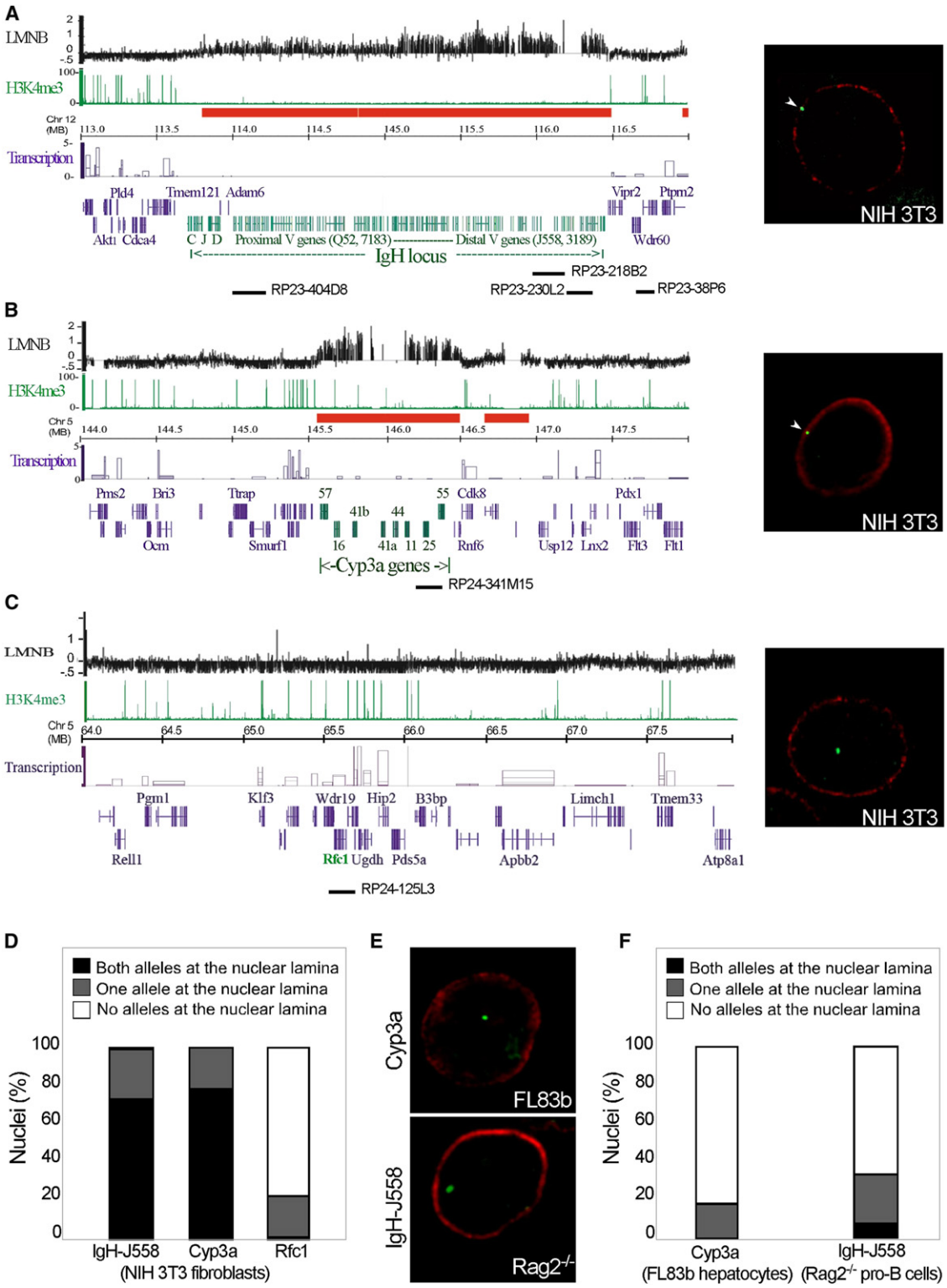

Figure 1. The *IgH* and *Cyp3a* Loci Comprise Developmentally Regulated LADs

(A–C) Dam-LMNB targeted methylation, H3K4me3 ChIPseq reads and RNA signal intensities for annotated chromosomal regions containing the *IgH*, *Cyp3a* and *Rfc1* loci in NIH 3T3 cells. Red bars represent LADs detected by the GADA algorithm. DamID tracks are presented as log2 ratios of methylation by Dam-LMNB relative to the Dam control. ChIPseq data are presented as number of reads for consecutive nonoverlapping genomic intervals. Transcription levels are derived from RNA hybridization signals using Affymetrix arrays. Right panels are representative images from 3D-ImmunoFISH using as probes the RP23-230L2 (*IgH*),

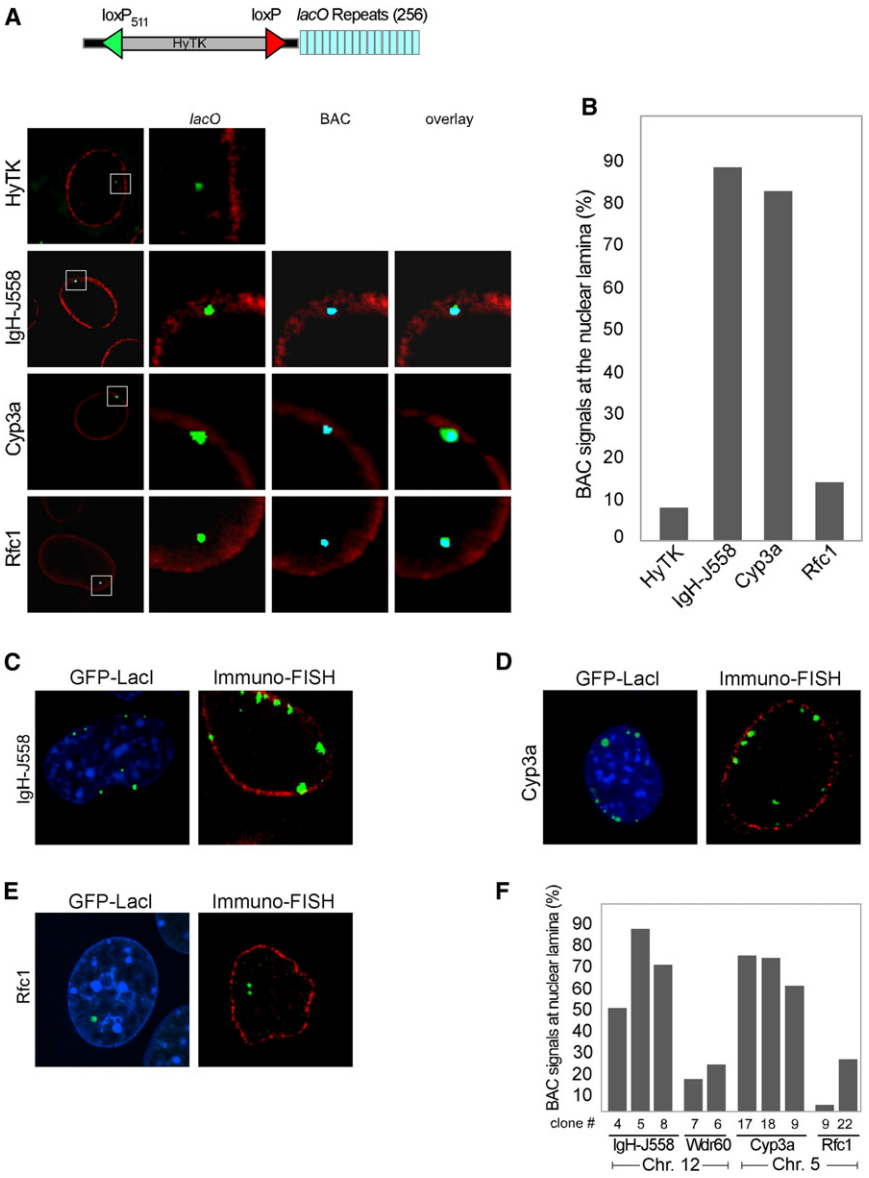

Figure 2. Ectopically Integrated LAD-Derived DNA Sequences Reposition Nucleoplasmic Chromatin to the Nuclear Lamina

(A) Site-specific integration and visualization of LAD-derived DNA sequences. Schematic of a construct containing a 256-copy *lacO* array and a *HyTK* fusion gene flanked by heterospecific and inverted loxP sites. NIH 3T3 cells with this construct stably integrated at a single insertion site that localized in the nucleoplasm (*HyTK*, top panels) were used for subsequent experiments. BACs bearing DNA sequences from the *IgH* (RP23-230L2) or *Cyp3a* (RP23-341M15) LADs or from a non-LAD control region *Rfc1* (RP24-125L3) were recombined into the *lacO* tagged insertion site and 3D-immunoFISH was used to visualize cointegration as well as the nuclear distribution of the integrated sequences as described in Figure 1.

(B) Quantitative analysis of the experiments described in (A).

(C–E) *IgH-J558*, *Cyp3a* or *Rfc1* BACs bearing the sequences indicated above were randomly co-integrated with *lacO* arrays into the genome of NIH 3T3 cells. Individual clones were analyzed for the subnuclear localization of the integrated sequences by fluorescence imaging of GFP-LacI foci (green) and Hoechst 33342 staining of nuclear DNA (blue) (left panels) and by 3D-ImmunoFISH using a pTARBAC vector DNA probe (green) and an anti-LMNB antibody (red) (right panels).

(F) Quantitative analysis of the experiments shown in panels C–E. The *Wdr60* BAC (RP23-38P6) was derived from a non-LAD region of chromosome 12 (Figure 1A). At least 100 nuclei from each cell clone were analyzed.

See also Figure S2.

assessed for their ability to reposition the chromosomal locus to the INM-lamina. The *lacO* repeats enabled visualization of the integration site in live cells that express LacI-GFP (Robinett et al., 1996). Given the sizes of LADs we initially tested large DNA regions for lamina positioning sequences. We used a bacterial artificial chromosome (BAC) derived from the 5′ region of the *IgH* locus (RP23-230L2, Figure 1A) because this domain of the endogenous locus had been suggested to associate with the lamina at a higher frequency (Kosak et al., 2002; Yang et al., 2005). For *Cyp3a*, we selected a BAC (RP24-341M15, Figure 1B) spanning one of eight genes in the cluster (*Cyp3a25*). The *Rfc1* BAC (Figure 1C) derived from a non-LAD region, was used as a negative control. Each of these BACs contained *loxP* sites, which enabled their integration into the tagged chromosomal site upon transient expression of Cre recombinase. We verified BAC cointegration with the *lacO* array by 3D-ImmunoFISH and then quantitatively analyzed the colocalization of these signals with the nuclear lamina (Figures 2A and 2B). Strikingly, DNA sequences from the *IgH* and

RP23-341M15 (*Cyp3a*), or RP24-125L3 (*Rfc1*) BAC DNAs. Genomic positions of all BACs used in this and subsequent experiments are displayed (black bars). Only one allele (green) per nucleus is shown in relation to the nuclear lamina (red).

(D) Quantitative analysis of 3D-ImmunoFISH images in panels A–C. Loci were considered to be at the nuclear lamina if part of the FISH signal overlapped with the that of lamin B.

(E and F) Analysis of nuclear positioning of *IgH-J558 and Cyp3a* alleles in *Rag2*−/− pro-B cells or Fl83b hepatocytes, respectively, as described for 3D-ImmunoFISH above. At least 100 nuclei were scored with each DNA probe.

See also Figure S1.

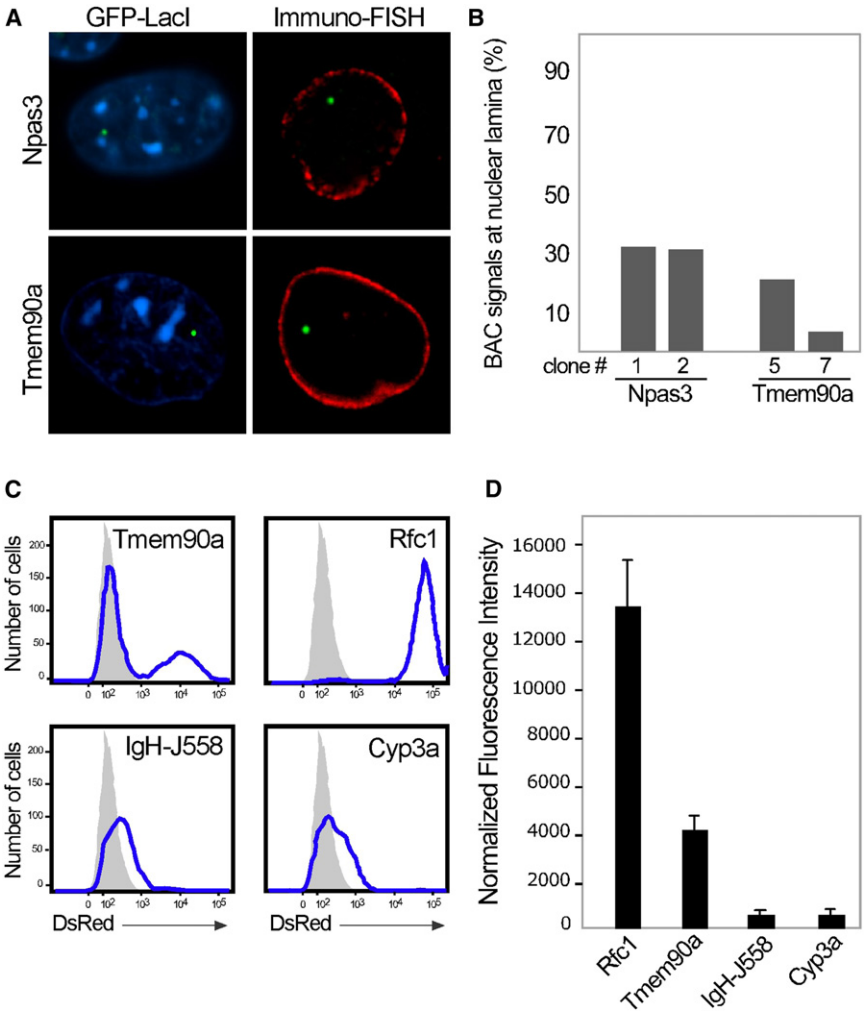

Figure 3. LAD-Derived DNA Sequences Repress Transcription

(A and B) Transcriptional inactivity is not sufficient to direct a chromosomal region to the INM-lamina. (A) BACs spanning transcriptionally inactive non-LAD regions containing the *Tmem90 gene* or the *Npas3 genes* (see Figure S3) were cointegrated with *lacO* arrays into the genome of NIH 3T3. Clones were analyzed for the subnuclear localization of the integrated sequences by fluorescence imaging of GFP-LacI (left panels) or by 3D-ImmunoFISH as in Figure 2. (B) Quantitative analysis of the experiments described in (A). At least 100 nuclei from each cell clone were analyzed.

(C and D) LAD-derived DNA represses transcription. (C) NIH 3T3 cells were cotransfected with BACs bearing the indicated chromosomal sequences and a plasmid containing the PGK-DsRed reporter gene. Stable cell lines were analyzed by flow cytometry for expression of DsRed protein (blue line). Grey histograms represent nontransfected NIH 3T3 cells. (D) The graph depicts mean DsRed fluorescence intensity for each of the designated BACs after normalization for DsRed plasmid copy number (determined by Q-PCR).

See also Figure S3.

Cyp3a LADs directed localization of the tagged chromosomal region to the nuclear lamina whereas the control sequence (*Rfc1*) did not. This was confirmed by visualizing GFP-LacI binding in live cells (data not shown). These results demonstrated that the *IgH* and *Cyp3a* LADs contain DNA regions that can reposition nucleoplasmic chromatin to the INM-lamina upon integration into an ectopic site.

To test if the lamina positioning property of these LAD-derived DNA regions was independent of the site of insertion we utilized a random integration assay. NIH 3T3 cells were cotransfected with the fore-mentioned *IgH* and *Cyp3a* BACs along with a plasmid harboring the *lacO* array. This resulted in random co-integration of LAD-derived sequences with *lacO* repeats. BACs from non-LAD regions encompassing the *Wdr60* (RP23-38P6, Figure 1A) or *Rfc1* (RP24-125L3, Figure 1C) genes residing on chromosomes 12 and 5, respectively, served as controls. Live cell imaging and 3D-ImmunoFISH were used to analyze the nuclear distributions of the integrated DNA sequences. Consistent with the site-specific assay, clones carrying insertions of either the *IgH* or *Cyp3a* LAD-derived DNA displayed a very high degree of lamina-associated signals (Figures 2C, 2D, and 2F). This was especially evident in clones with multiple genomic insertions. In contrast, DNA sequences derived from the non-LAD regions *Rfc1* and *Wdr60* primarily localized to the nucleoplasm (Figures 2E and 2F). To determine if the *IgH* LAD contains multiple regions that are capable of associating it with the nuclear lamina, two additional BACs, one drawn from the 5′ distal *Vh* region (RP23-218B2) and the other from the 3′ proximal *Vh* region (RP23-404D8) were tested (Figure 1A and Figure S2). Intriguingly, both of these regions were capable of targeting chromosomal domains to the nuclear lamina, although the *IgH* 3′ sequence displayed reduced levels of association. Thus the *IgH* and *Cyp3a* LADs contain DNA regions that can direct the interaction of chromatin with the INM-lamina upon integration at ectopic sites.

LAD-Derived DNA Mediates Transcriptional Repression

As the genes encoded in the two non-LAD regions are actively transcribed in NIH 3T3 fibroblasts, the possibility remained that the positioning of LAD-derived DNA at nuclear lamina was simply a reflection of its inactive transcriptional state. To rigorously rule out this possibility, we performed the nuclear positioning assay using two non-LAD-derived regions, containing the *Tmem90a or Npas3* genes, which are not transcribed in fibroblasts (Figure S3). Importantly, upon random integration, these inactive non-LAD regions were predominantly localized to the nucleoplasm (Figures 3A and 3B) just as their transcribed non-LAD counterparts (Figures 2E and 2F). Thus, positioning of chromatin

domains at the nuclear lamina is not simply the property of a transcriptionally inactive state but appears instead to be directed by specific DNA regions within LADs.

To determine if repositioning of chromatin mediated by LAD-derived sequences results in transcriptional repression, we utilized a reporter construct encoding the DsRED gene under the control of the murine phosphoglycerate kinase (PGK) promoter. The reporter plasmid was cotransfected into NIH 3T3 fibroblasts with lamina-targeting *IgH* or *Cyp3a* LAD-derived BACs, or control non-LAD-derived BACs. We confirmed the expected nuclear positions of the LAD and non-LAD sequences as well as their cointegration with the DsRED plasmid by 3D-ImmunoFISH (data not shown). The effect of lamina association on DsRED expression was then examined by fluorescence activated cell sorting (Figures 3C and 3D). Positioning of the DsRED gene at the nuclear lamina via cointegration with the *IgH* or *Cyp3a* sequences resulted in uniformly reduced levels of expression, whereas cointegration of the *Tmem90a* non-LAD region with the reporter plasmid resulted in a bimodal distribution of DsRED expression, presumably as a consequence of position effects resulting from different integration sites. Notably, the *Rfc1* BAC, which is contained within an actively transcribed, non-LAD region, resulted in homogeneously high DsRED expression. Thus, positioning of an actively transcribed gene at the nuclear lamina, via a LAD-derived DNA sequence, results in its transcriptional repression and overrides position effect variation.

Mitosis Is Required for Interaction of LAD-Derived DNA with INM-Lamina

The positioning of the *CFTR* locus at the nuclear periphery has been shown to be sensitive to histone deacetylase inhibitors (Zink et al., 2004). Therefore we tested the effect of trichostatin A (TSA) on the nuclear compartmentalization of ectopically inserted LAD-derived DNA. TSA treatment of the cells harboring the integrated *IgH* and *Cyp3a* BACs resulted in their dissociation from the nuclear lamina (Figures S4A and S4B). We note that TSA treatment also induced the release of the endogenous *IgH* and *Cyp3a* loci from the INM-lamina (Figures S4C and S4D). Importantly, lamina association was reversible; within 24 hr of TSA withdrawal the loci resumed their position at the INM-lamina.

Given that TSA treatment could be used to modulate the interactions of LAD-derived sequences with the nuclear lamina, we used it as a tool to explore the dynamics of dissociation and re-association of LADs in the context of the cell cycle. To test if the release of LAD-derived sequences from the nuclear lamina can occur in the absence of mitosis we pretreated cells bearing the *Cyp3a* BAC with the DNA replication inhibitor aphidicolin prior to the addition of TSA. The results demonstrated that release of LAD-derived sequences from the INM-lamina does not require passage through mitosis. However, re-association was inhibited by aphidicolin-mediated cell cycle arrest (Figures S4A and S4B). These results suggested that association of LADs with the lamina occurs during mitosis.

To further analyze the basis of LAD association with the nuclear lamina, we examined the interaction of the lamina-targeting BACs with LMNB during mitosis in synchronized cell populations. Interestingly, in prophase, after dissolution of the nuclear lamina, the GFP-LacI foci marking the *Cyp3a* BAC integrations were situated at the periphery of the condensing chromosomal regions (Figure 4A). In contrast, the non-LAD *Tmem90a* sequence localized to the interior of the condensed chromosome throughout mitosis (Figures 4B and 4D). At the end of anaphase, as the lamina begins to reform around chromatin, we observed a striking colocalization of LMNB with the LAD-derived sequences (Figure 4C). The ability to readily detect these LMNB foci at sites of ectopic LAD DNA integration is likely due to multicopy insertions of the LAD-derived sequences. We did not observe colocalization of LAD-derived regions with Nup153 (Figure 4E), a component of the nuclear pore complex (NPC) that also associates with chromatin during late anaphase. Thus the accumulation of LMNB on LAD-derived DNA sequences at the end of anaphase likely reflects a specific interaction, rather than simply being a consequence of the peripheral positioning of LADs in mitotic chromosomes.

Delineation of Lamina-Associating Sequences

To delineate DNA sequences that function in tethering chromatin to the nuclear lamina we tested smaller fragments (12–32 kb) generated from the *IgH* or *Cyp3a* BACs described above. These fragments were individually cointegrated with *lacO* arrays and then analyzed for lamina localization (Figure 5A and Figure S5A). Many of these fragments (green bars) exhibited a high degree of lamina association. Next, smaller segments (4–6 kb) were analyzed. Once again, many of these subfragments displayed a high degree of lamina association (Figure 5A and Figure S5B). We term these DNA fragments lamina-associating sequences (LASs). The MEME algorithm was used to conduct de novo motif analysis of LASs (Bailey, 1994). The highest scoring motif (E value = 9.1×10^{9}) was composed primarily of GA dinucleotides (Figure 5B, lower sequence in top panel). Importantly, the frequency of occurrence of this extended GAGA motif was much higher in the BAC-derived fragments with high lamina association scores compared to those that exhibited lower levels of lamina association (Figure S5C). Furthermore, it was enriched within LADs relative to non-LAD regions on chromosomes 5, 12, and 15 (p value 1×10^{-7}). Thus LADs contain numerous and dispersed LASs, which are enriched for an extended GAGA motif.

cKrox and HDAC3 Are Required for Lamina Association

The extended GA dinucleotide motif was predicted by TomTom (Bailey, 1994) to be recognized by the GAGA transcription factor (Figure 5B, upper sequence in top panel). This factor performs multiple genome-regulatory functions in *Drosophila*, including the assembly of heterochromatin (Adkins et al., 2006). Recently, cKrox (ThPOK) has been identified as the vertebrate ortholog of the GAGA factor and shown to have a similar DNA-binding specificity (Matharu et al., 2010). cKrox contains a conserved BTB/POZ domain, which enables transcriptional repression through interaction with HDAC-containing N-CoR/SMRT complexes (Melnick et al., 2002). As HDAC3 has been shown to interact with the INM protein Lap2β (Somech et al., 2005), we hypothesized that cKrox could promote association of chromatin with the nuclear lamina by binding to the GAGA motifs in

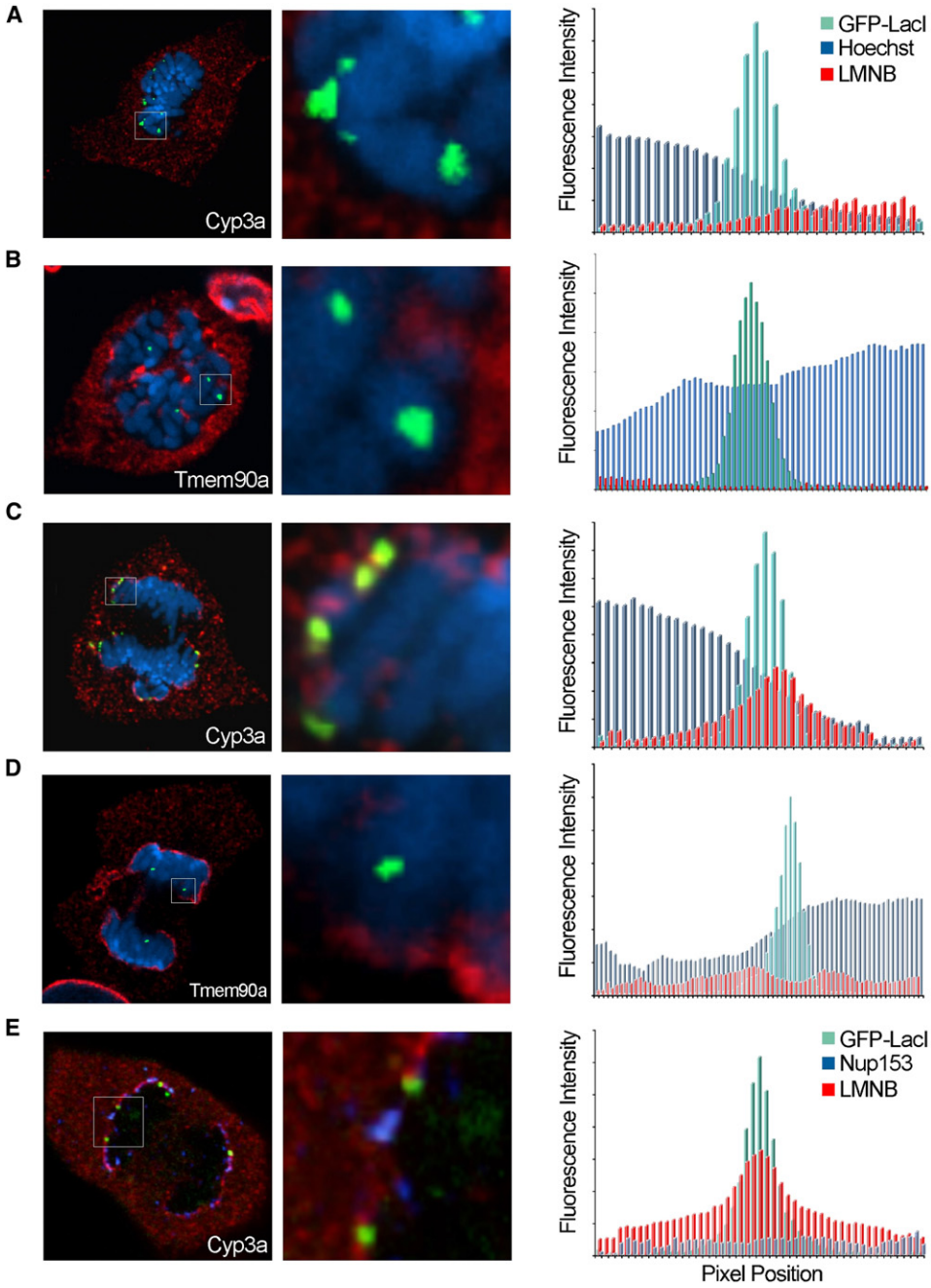

Figure 4. LAD-Derived Sequences Interact with the Nascent Lamina during Late Anaphase

Cells from NIH 3T3 lines expressing GFP-LacI and bearing multiple insertions of *lacO* arrays and the indicated BACs were arrested in S phase using aphidicolin (12h). After release from the aphidicolin block (6.5h), cells were fixed and stained with an antibody against LMNB (red) and Hoechst 33342 (blue) (A–D), or antibodies against LMNB (red) and Nup153 (blue) (E). Representative images for cells undergoing prophase (A and B) or anaphase (C–E) are shown (left panels). Each image displays the positioning of *lacO* foci (green) revealed by GFP-LacI binding in relation to either condensed chromosomal DNA and LMNB domains (A–D) or to that of Nup153 foci and LMNB domains (E). The fluorescence intensity profiles for LMNB and Hoechst or LMNB and Nup153 in relation to GFP-LacI foci were analyzed by quantitative image analysis (right panels). Linear intensity profiles were aligned using their GFP maxima, such that each plot shows the averaged distribution of intensities on each fluorescent channel from at least 30 mitotic figures. See also Figure S4.

LASs and recruiting HDAC3 to enable both histone deacetylation and interaction with an INM protein. We generated nuclear extracts from NIH 3T3 cells transfected with a Myc-tagged cKrox expression plasmid and utilized electrophoretic mobility shift assays (EMSAs) to determine whether cKrox binds to the GAGA motifs contained in the *IgH* and *Cyp3a* LASs.

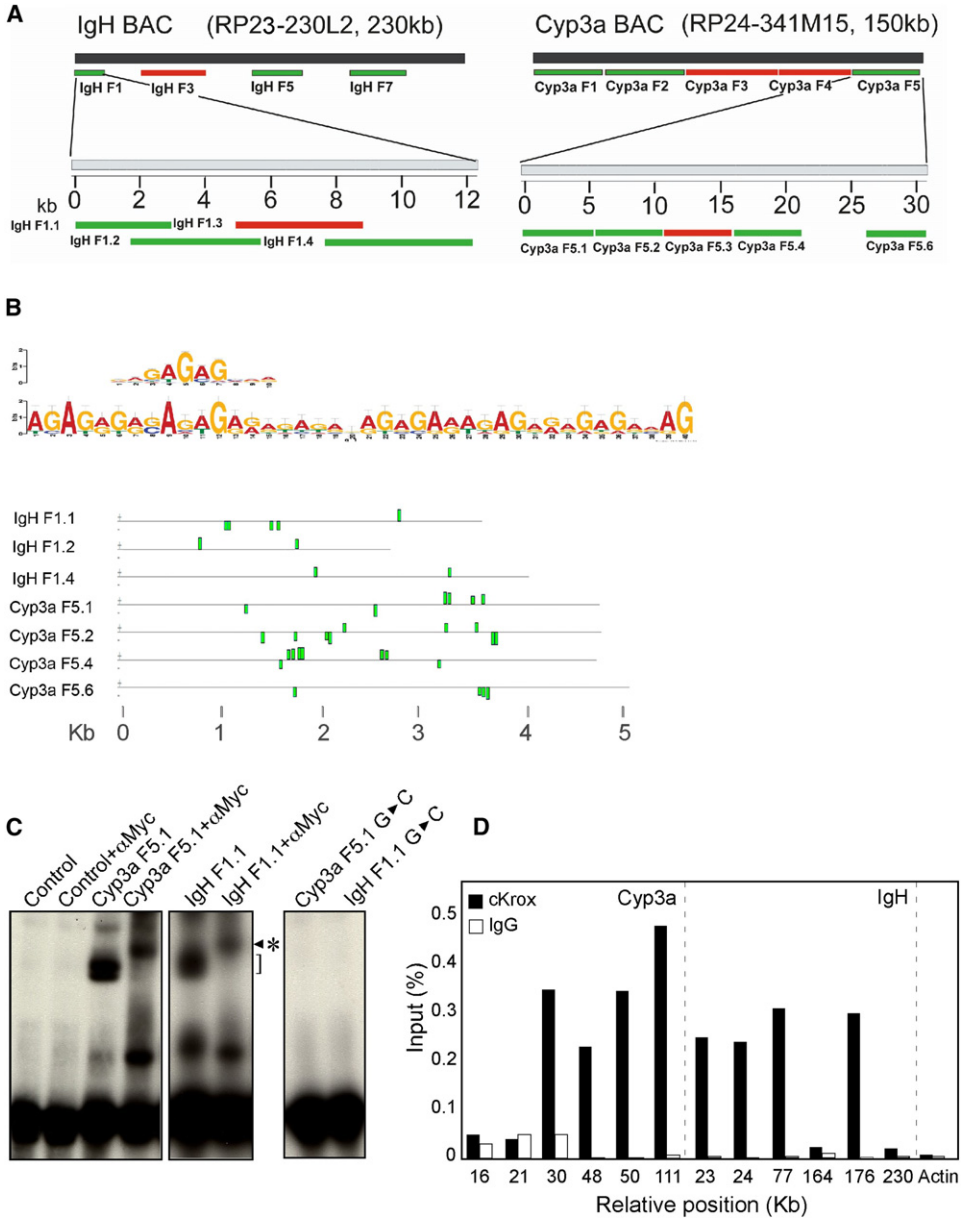

Figure 5. Delineation of Lamina-Associating Sequences

(A) The depicted subfragments (12-32kb) were derived from RP23-230L2 (*IgH*) or RP24-341M15 (*Cyp3a*) BACs. 3D-ImmunoFISH was used to analyze the nuclear localization of these integrated sequences. Green bars indicate fragments with a high degree of INM-lamina association (>60%) with respect to the control *lacO* DNA (<35%). Red bars indicate fragments that displayed INM-lamina association at levels observed with control DNA. The fragments with the highest degree of INM-lamina association (*IgH* F1 and *Cyp3a* F5) were subdivided and analyzed as above.

(B) MEME analysis of LASs reveals an extended GA-rich motif (lower sequence, top panel). The upper sequence in the top panel depicts the binding site matrix for cKrox in the Transfac database. Bottom panel displays the occurrence and distribution of extended GAGA motifs (green boxes) in the indicated LAS fragments. The height of the green bars is a measure of the relatedness of the extended GAGA motif sequence marked by the box to the one displayed in the upper panel.

(C) Gel shift assays using nuclear extracts from NIH 3T3 cells expressing Myc-tagged cKrox. Control, wild-type and mutated oligonucleotides used as DNA probes are indicated. The GAGA motif was altered to CACA in the mutant probes. Protein/DNA complexes (bracket) that were supershifted by the addition of an anti-Myc antibody are indicated with an asterisk.

(D) ChIP assay analyzing the binding of cKrox to GAGA motif containing sequences within the *IgH* and *Cyp3a* loci in NIH 3T3 cells. The relative positions of the GAGA motif sequences in the *IgH* and *Cyp3a* BACs, RP23-230L2 and RP24-314M15, respectively, are indicated. An α-actin gene segment lacking the GAGA motif and an isotype matched IgG antibody were used as controls. The extent of cKrox bound DNA sequence is displayed as a fraction of the input chromatin. See also Figure S5 and Tables S2 and S4.

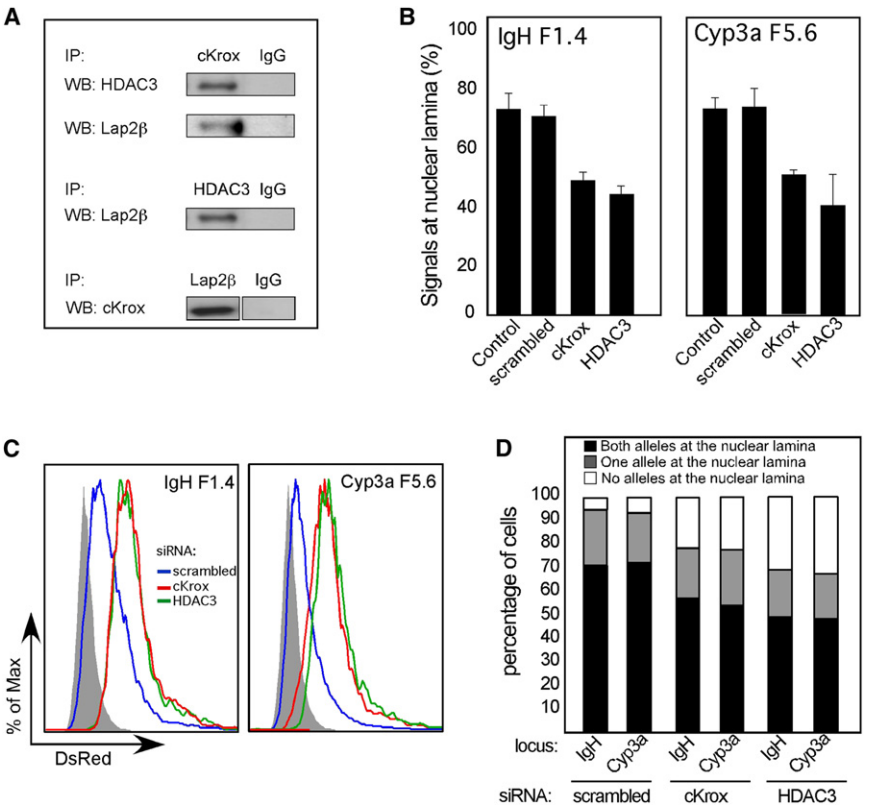

Figure 6. cKrox Interacts with HDAC3 and Lap2β to Promote Chromatin Association with the Lamina

(A) Nuclear lysates from NIH 3T3 cells were used for immunoprecipitation (IP) with α-cKrox, α-HDAC3, or α-Lap2β, followed by western blotting (WB) using indicated antibodies.

(B) Cell lines bearing indicated LASs were transiently transfected with siRNAs directed against cKrox, HDAC3 or controls. Knockdown of the targeted protein was verified by WB (Figure S6). Nuclear distribution of the LAS was analyzed as in Figure 5.

(C) Cell lines bearing either IgH F1.4 or Cyp3a F5.6 LAS and a cointegrated PGK-DsRed reporter gene were transfected with the indicated siRNAs as described in (B). After 56 hr, DsRed expression was analyzed by flow cytometry. Gray histograms represent control NIH 3T3 cells.

(D) NIH 3T3 fibroblasts were transfected with the indicated siRNAs as described in (C). The nuclear localization of *IgH* and *Cyp3a* loci was analyzed after 56 hr as detailed in Figure 1. At least 100 nuclei were scored for each condition.

See also Figure S6 and Table S3.

Protein-DNA complexes were detected with GAGA motif-bearing oligonucleotides derived from four distinct LASs but not with a control sequence (Figure S5D). The complexes were supershifted with an anti-Myc antibody and were not formed if the GAGA motif was mutated to CACA (Figure 5C). ChIP analysis confirmed the binding of endogenously expressed cKrox to multiple LASs within the *IgH* and *Cyp3a* loci (Figure 5D). These results demonstrate that cKrox binds in vitro as well as in vivo to the GAGA motif within LASs.

To test additional aspects of our molecular hypothesis, we analyzed protein-DNA complexes that assembled on GAGA motifs by DNA affinity capture and immunoblotting. Both cKrox and HDAC3 were observed to associate with the GAGA motif-containing oligonucleotides (Figure S5E). Immunoprecipitation of cKrox revealed its association with HDAC3 and Lap2β (Figure 6A). The interactions among these three proteins were further supported by the association of HDAC3 with Lap2β and of the latter with cKrox. Thus cKrox binds GAGA motifs in LASs and interacts with HDAC3 as well as Lap2β, suggesting that this complex may be utilized in both the association of chromatin domains with the nuclear lamina as well as their transcriptional repression.

To test this model, we performed siRNA knockdown experiments targeting cKrox and HDAC3 in NIH 3T3 cells bearing LASs from the *IgH* or *Cyp3a* loci (Figure 6B). Western blotting was used to confirm the reduced expression of cKrox and HDAC3 in the siRNA-transfected cells (Figure S6A). Knockdown of either protein showed a marked effect on the ability of LASs to be retained at the lamina and also resulted in transcriptional de-repression of a reporter gene that was cointegrated with these LASs (Figures 6B and 6C). Importantly, these perturbations also reduced the number of endogenous *IgH* and *Cyp3a* alleles that were associated with the INM-lamina (Figure 6D). We note that knockdown of Lap2β had dissimilar effects, depending on which of the two LASs were assayed and had a less pronounced effect on the localization of the endogenous loci. These results suggest that a cKrox-HDAC3 complex, interacting with Lap2β and likely additional INM proteins is required for LAS association with the INM-lamina.

We also tested for the involvement of BAF in the association of LASs with the nuclear lamina. This abundant chromatin binding protein interacts with INM components such as Lap2β and emerin as well as with transcription factors and could function as a bridging molecule (Margalit et al., 2007). However, knockdown of BAF did not affect the association of the *IgH* or *Cyp3a* LASs with the nuclear lamina (Figure S6B).

To analyze whether the extended GAGA motif is sufficient to target genomic regions to the INM-lamina, we generated 400 bp tandem arrays containing ten copies of either a wild-type or mutated GAGA motif and inserted them into the *lacO* array vector. When integrated into the genome of NIH 3T3 cells, the *lacO* vector containing the wild-type GAGA motif showed a marked increase in colocalization with the INM-lamina (Figure 7A). In contrast, the vector containing a CACA motif was localized predominantly at the nuclear interior, similar to the parental control.

Next, we sought to determine whether the interaction between cKrox and LASs is established during nuclear

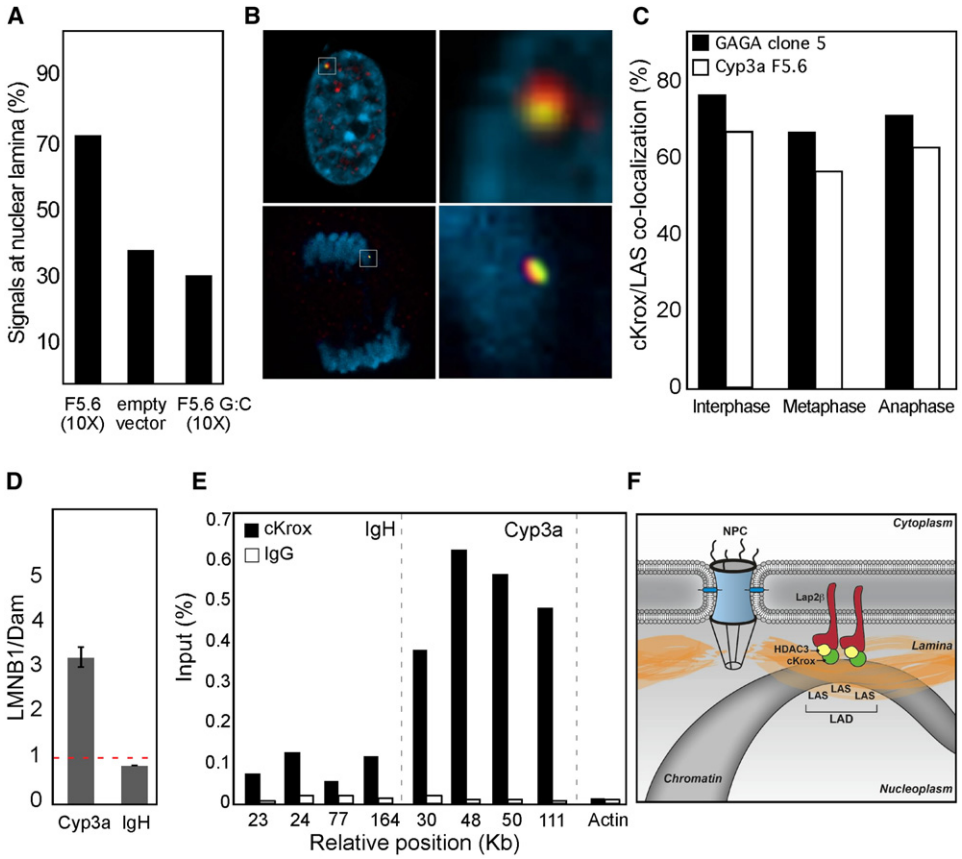

Figure 7. cKrox Mediates Association of Chromatin with the INM-Lamina via the GAGA Motif

(A) *lacO* vectors bearing tandem copies (10) of the wild-type GAGA motif derived from *Cyp3a* F5.6 or its mutant CACA (G→C) counterpart were analyzed for nuclear positioning after integration into the genome of NIH 3T3 cells. Quantitative analysis of signals at the nuclear lamina was performed as in Figure 5.

(B) Cells carrying the GAGA array described above were arrested in S phase using aphidicolin. After release from the block, cells were fixed and stained with Hoechst 33342 (blue) and an antibody against cKrox (red). Representative images for cells in interphase (top panels) or anaphase (bottom panels) are shown. Each image displays the positioning of *lacO* foci (green) revealed by GFP-LacI binding in relation to chromosomal DNA and cKrox foci. Right panels show a magnification of the highlighted areas in the left panels.

(C) Quantitative analysis of the experiment described in (B) using cell lines carrying either the GAGA array or the *Cyp3a* F5.6 LAS.

(D) Interaction of LMNB1 with the *IgH* and *Cyp3a* loci in *Rag2*−/− pro-B nuclei detected by DamID-mediated methylation followed by quantitative PCR. The *Cyp3a* primers amplify a segment of the *Cyp3a57* gene within the cluster. The *IgH* primers amplify a distal *J558a* V_H promoter segment (also see Figure S7). Signals were normalized to a Dam only control as in Figure 1.

(E) ChIP assay analyzing the binding of cKrox to GAGA motif-containing sequences within the *IgH* and *Cyp3a* loci in *Rag2*−/− pro-B cells. See Figure 5D for details.

(F) Model depicting the interaction of multiple LASs in a LAD with the INM-lamina. GAGA motifs in LASs are recognized by cKrox, which interacts with HDAC3 and the INM protein Lap2β. HDAC3 is proposed to function both as an adaptor for lamina association as well as a transcriptional corepressor via its histone deacetylase activity.

See also Figure S7 and Table S4.

envelope reformation, concomitant with the observed association of LASs with the assembling nuclear lamina during late anaphase (Figure 4). In cell lines carrying either the *Cyp3a* F5.6 LAS or the GAGA motif arrays, cKrox colocalized with the inserted DNA sequences at the INM-lamina in a large proportion of the cells (Figure 7B, top panels). Intriguingly, cKrox was also seen to be associated with the integrated sequences throughout mitosis (Figure 7B, bottom panels). The latter results suggest that cKrox remains bound to LASs throughout mitosis and therefore precedes the association of LASs with the nuclear envelope in late anaphase.

Developmental Control of LAS Activity

To analyze the developmental control of LAS activity we sought to determine if cKrox remains bound to LASs in the *IgH* locus in pro-B cells, where this locus is released from the nuclear lamina and activated for transcription (Bertolino et al., 2005). Consistent with its nucleoplasmic positioning, DamID mapping of chromosome 12 in *Rag2*−/− pro-B cells showed that the *IgH* locus was not included in a LAD (Figure S7). DamID analysis of sequences within the *IgH* locus versus the *Cyp3a* cluster showed that the latter were still associated with the nuclear lamina in pro-B cells (Figure 7D). Thus, whereas both loci interact

with the nuclear lamina in fibroblasts, the *IgH* locus is selectively released from the lamina in pro-B cells. *Rag2*−/− pro-B cells express cKrox at levels comparable to those observed in fibroblasts (data not shown). ChIP assays showed that cKrox binding was substantially lower at LASs within the *IgH* locus compared with LASs within the *Cyp3a* cluster (Figure 7E). Thus the binding of cKrox to LASs appears to be under developmental control and is regulated in a locus specific manner. Furthermore loss of cKrox binding to LASs within the *IgH* locus is correlated with its transcriptional activation and release from the nuclear lamina.

DISCUSSION

Distinct molecular mechanisms have been proposed to account for the interaction of inactive chromatin domains with the nuclear lamina (Kind and van Steensel, 2010). We have utilized genomic repositioning assays to demonstrate that DNA sequence, and not transcriptional inactivity or chromosomal location, is the primary basis by which chromatin is targeted to the nuclear lamina. Within the *IgH* and *Cyp3a* LADs our analysis identified multiple dispersed elements termed LASs that are capable of promoting association of chromatin with the nuclear lamina and transcriptional repression. This distinctive nuclear compartmentalization appears to be mediated by a protein complex that contains cKrox, HDAC3, and Lap2β and recognizes extended GAGA motifs (Figure 7F). We note that transcriptional silencing of genes via recruitment to the nuclear envelope has also been observed in yeast (Taddei et al., 2010), although their nuclei lack lamins and many of the INM proteins found in mammalian cells. Attachment of telomeric DNA to the nuclear envelope in yeast is mediated by the transcription factor Rap1 that binds the TG repeat sequence and recruits the SIR chromatin-modifying complex to repress gene activity. Sir4 interacts with Esc1, which functions as a perinuclear anchor (Taddei et al., 2004). Thus mechanisms utilizing a similar molecular logic appear to be involved in the recruitment and silencing of yeast and mammalian genes at the nuclear envelope.

In contrast with the above, a DNA-based mechanism of gene targeting to nuclear pore complexes (NPCs) that functions in promoting transcription has been recently delineated in yeast (Ahmed et al., 2010). This analysis revealed two short motifs, either of which is sufficient for recruitment of chromatin to the yeast NPC. These results in yeast are consistent with various reports in flies and mice describing the NPC as a subcompartment that promotes gene expression (Brown and Silver, 2007). Thus distinct DNA "address" signals that direct nuclear subcompartmentalization are likely to be found within diverse eukaryotic genomes and represent a widespread means of regulating genome activity and function.

Previous results from our laboratory and those of others have shown that inducible tethering of a reporter gene to the INM-lamina using synthetic elements results in transcriptional repression (Finlan et al., 2008; Reddy et al., 2008). The current experiments demonstrate that native mammalian sequences (LASs) can mediate attachment of a reporter gene to the nuclear lamina and its transcriptional silencing. Transcriptional repression by LASs is likely to be induced by selective alterations in histone modifications mediated by enzymes that reside within the INM-lamina. Given our demonstration that the chromatin remodeling enzyme HDAC3 is required for localization of LASs to the lamina, we propose that localization to the lamina and histone deacetylation, which is associated with transcriptional repression, are likely to be mechanistically coupled. Intriguingly, knockout of HDAC3 in hepatocytes has been shown to result in a dramatic loss of much of the heterochromatin, which is associated with the nuclear envelope (Bhaskara et al., 2010). These results complement our findings and reinforce a major function for HDAC3 in establishing and/or maintaining heterochromatin at the INM-lamina. The issue of whether the catalytic activity of HDAC3 is required for lamina association remains to be addressed. HDAC3 could promote lamina association via its interaction with cKrox and Lap2β and also via histone deacetylation that facilitates binding of heterochromatin proteins, which in turn interact with additional INM-lamina components. We note that a recent study has identified H3K9me2 as a repressive histone mark that may be associated with LADs (Wen et al., 2009). Depletion of this histone mark by knocking out G9a methyltransferase alleviates transcriptional repression without affecting nuclear localization (Yokochi et al., 2009). Therefore, gene positioning at the INM-lamina and its associated repressive chromatin state can be experimentally uncoupled. The potential molecular interplay between HDAC3-mediated histone deacetylation and G9a-mediated histone methylation in establishing as well as maintaining transcriptional repression of chromatin at the nuclear lamina needs to be explored further.

An emerging principle observed in histone modifying complexes is the presence of protein domains that perpetuate feed-forward loops. For example, the HDAC-interacting corepressors N-CoR and SMRT contain SANT domains that promote binding to deacetylated histone tails, the inhibition of histone acetyltransferase (HAT) activity and the stimulation of HDAC3 activity (Yu et al., 2003), thereby augmenting N-CoR/SMRT action. Additionally, canonical heterochromatin proteins such as HP1β recruit transcriptional corepressors, are associated with the INM, and require HDAC3 activity to bind chromatin (Bhaskara et al., 2010). Such HDAC3-dependent, self-reinforcing interactions could be important in spreading a repressive chromatin state, explaining how relatively small, dispersed sequences could silence large spans of genomic DNA to create LADs.

Our data indicate that LASs interact with the nascent lamina in late anaphase during nuclear envelope reformation. A possible mechanistic explanation for this phenomenon may be that regions containing LASs serve as points of nucleation for LMNB and INM proteins. Such a process would simultaneously facilitate nuclear envelope reassembly as well as the compartmentalization of these regions into repressive chromatin domains, which would then persist in interphase. An intriguing implication of this observation is that LASs may be utilized to ensure the enclosure of a complete set of segregated chromosomes by the newly formed nuclear envelope of a daughter cell resulting from a mitotic division. Indeed, the *Drosophila* ortholog of cKrox (GAF) is required for proper chromosome segregation (Bhat et al., 1996). Consistent with this possibility, many LADs do not contain genes and appear to constitutively

associate with the lamina (Peric-Hupkes et al., 2010). Such constitutive LADs and their embedded LASs may serve a structural role as scaffold elements for chromosomes during nuclear envelope reassembly as well as organizers of the genome during interphase.

How INM-lamina components are recruited to LASs during late anaphase remains to be elucidated. Intriguingly, we observe foci of both Lamin B and cKrox associated with integrated multicopy LASs during late anaphase. Moreover, cKrox is associated with these LASs throughout mitosis. Thus it is possible that cKrox enables localized lamin B deposition during late anaphase. In this way, cKrox retained on mitotic chromatin may constitute a molecular memory of LADs from the preceding interphase, that enables their re-establishment following cell division. Since we detected cKrox foci associated with mitotic chromatin while only using integrated arrays that contain a large number of cKrox binding sites, we propose that a small number of cKrox molecules bound to native LASs in mitotic chromatin may be sufficient to promote the association of LASs with the lamina during nuclear envelope reassembly. It will be important to determine the order of assembly of various molecular components such as HDAC3 and Lap2β on LASs during mitosis and the means by which this process is coordinated with reformation of the nuclear envelope. Finally, the generality of our proposed molecular mechanism (Figure 7F) remains to be explored. Based on our siRNA knockdown data, we suggest other INM proteins function redundantly with Lap2β to mediate LAS-lamina interactions and LAD formation Furthermore, cKrox, while broadly expressed, is not ubiquitous, it is likely that there exists a class of mammalian transcriptional repressors that act in analogous fashion to facilitate interaction with the lamina.

cKrox (ThPOK) was initially cloned as a transcription factor expressed in fibroblasts and suggested to function in the repression of the *collagen a1* gene (Galéra et al., 1994). Subsequently it has been shown to be a key regulator of CD4 versus CD8 T cell fate choice in the thymus (He et al., 2010), initiating and maintaining the repression of the alternate lineage CD8 locus in CD4 T cells. cKrox appears to repress gene activity through its interactions with the HDAC3-interacting N-CoR/SMRT complexes. We note that cKrox is closely related to LRF/Pokemon and Apm-1, therefore these transcription factors may also function in LAS-mediated gene repression. As noted earlier, cKrox is the vertebrate ortholog of the *Drosophila* GAGA factor. Interestingly, GAF associates with pericentromeric heterochromatin that contains GA repeats (Raff et al., 1994), mediates polycomb-mediated gene silencing, and functions to establish chromatin boundaries (Bhat et al., 1996). It will be important to explore if any of these functions of GAF are conserved in cKrox and if they are the consequence of an ability to associate chromatin domains to the nuclear lamina.

LADs that contain cell-type-specific genes such as the *IgH* and *Cyp3a* loci must have their function constrained by developmental cues. Importantly, we show that the binding of cKrox to LASs is developmentally regulated in a locus specific manner. Therefore, a means for overriding LAS function could involve the displacement of the cKrox tethering complex by the action of one or more transcription factors that function in cell fate determination. Given the large size of LADs and the prevalence of LASs, this could require that the pivotal transcription factor(s) bind at multiple sites in close proximity to LASs to destabilize or compete away cKrox/HDAC3 complexes. Alternatively, such transcription factors could achieve a similar effect by binding a few sites and propagating a large-scale change in chromatin structure by recruitment of remodelers and initiation of transcription. Indeed, multiple germline transcripts are seen to originate from the *IgH* locus concomitant with its repositioning into the nucleoplasm in B-lineage cells (Bolland et al., 2004). Further molecular analysis of the assembly and disassembly of LAS-bound tethering complexes described herein, in specific cellular contexts, will be needed to gain deeper insight into the developmental control of LAD organization and function.

EXPERIMENTAL PROCEDURES

DamID

DamID was performed as described previously (Reddy et al., 2008; Vogel et al., 2007) with some modifications to enable analysis by tiling arrays. Genomic DNA was isolated from transduced cells using QIAGEN DNeasy kit and PCR ligation-mediated amplification involved 18 cycles. Amplified DNA was fragmented by UDG/APE treatment. Hybridizations of the DamID samples were performed on separate Affymetrix Mouse genome 2.0 E chips as per manufacturer recommendations. Probe intensity ratios between Dam-LMNB fusion constructs and Dam alone were obtained using Affymetrix Tiling Array Analysis Software tools. All experiments were performed at least two independent times.

ChIPseq

NIH 3T3 cells were cultured as described and fixed with formaldehyde for ChIPseq analysis using antibodies recognizing H3K4me3, H3K27me3, H3K36me3 or CTCF (see Extended Experimental Procedures).

Bioinformatic Analyses of DamID and ChIPseq Data

DamID data were analyzed using the GADA algorithm (Pique-Regi et al., 2008) in order to delineate LADs (see Extended Experimental Procedures). The enrichment analysis for histone modifications or CTCF binding was performed by aligning 40 kb DNA tracts that flanked 144 LAD boundaries. Within these 40 kb regions, ChIPseq signal intensity peaks were then called by counting the number of 25 bp reads in 2 kb windows for the indicated ChIP target and comparing them to the read counts from the whole cell extract (WCE) background. Windows containing read counts at least ten-fold higher than WCE were considered peaks in the enrichment analysis.

Bacterial Artificial Chromosomes

All BACs were obtained from the BACPAC Resource Center at Children's Hospital Oakland Research Institute (Oakland, CA). The listing of the BACs with their NCBI clone-IDs and the genes they contain is provided in Table S1. These BACs can be displayed against the most current build of the genome at http://www.ncbi.nlm.nih.gov/genome/clone/.

Plasmids Used for Nuclear Compartmentalization Analysis

The *Tk-hyg lacO* and GFP-LacI plasmids have been described previously (Reddy et al., 2008). The TCIS vector was constructed by flanking a hygromycin phosphotransferase-thymidine kinase fusion gene (*HyTK*) by a wild-type loxP and a heterospecific loxP (loxP511) site. Subsequently, a 256-repeat *lacO* array was integrated upstream of the loxP511 site.

Generation and Propagation of NIH 3T3 Cell Lines and Clones

NIH 3T3 murine fibroblasts were transduced with the GFP-LacI retroviral vector and selected with puromycin (1 μg/ml) to generate a derivative expressing GFP-LacI. For site-specific BAC recombination experiments, the NIH 3T3 cell line expressing GFP-LacI was transfected with the linearized TCIS construct described above. Cells were selected for hygromycin resistance

(500 μg/ml) and clones were isolated and expanded. Integration events were analyzed by GFP-LacI fluorescence, and a clone displaying a *lacO* insertion at a single chromosomal site positioned away from the nuclear lamina (TCIS clone 2) was utilized for subsequent experiments. Site-specific recombination was achieved by cotransfecting TCIS clone 2 cells with the described BACs and a vector encoding for the Cre recombinase. Cells resistant to ganciclovir (10 μM) were selected and expanded for analyses of nuclear positioning of the integrated DNA sequences. For analyses of nuclear targeting by random integration, the parental GFP-LacI cell line was cotransfected with the indicated linearized BACs and *Tk-hyg lacO* at a 10:1 ratio (by weight). Cells were selected for hygromycin resistance as above. All transfections were performed using the Effectene transfection reagent (QIAGEN). Clones were isolated using cloning cylinders. Cells were expanded and maintained in DMEM with 10% FCS in the presence of hygromycin (500 μg/ml) and IPTG (2 mM). To enable binding of GFP-LacI, IPTG was washed out of the culture medium and cells were analyzed after 24 to 48 hr.

Live Cell Imaging and Immunofluorescence

Cells were prepared for live cell imaging by plating on 25 mm round coverslips or glass-bottom multi-well plates (MatTek). Images were obtained by laser scanning confocal microscopy using an Olympus Fluoview 1000 equipped with an environmental chamber to keep cells under physiological conditions. For immunofluorescence, cells were grown on sterilized 25 mm round coverslips (Deckglaser) in 6 well plates. The nuclear lamina and NPC were visualized using anti-LMNB and anti-Nup153 antibodies, respectively (see Extended Experimental Procedures).

3D DNA-ImmunoFISH

Immunofluorescence coupled with fluorescent DNA in situ hybridization on preserved nuclei (3D-ImmunoFISH) was performed as described previously (Reddy et al., 2008). DNA hybridization probes were generated by nick translation in the presence of digoxigenin or biotin-conjugated nucleotides (see Extended Experimental Procedures). After probe hybridization an anti-LMNB antibody was used to visualize the disposition of a given DNA region in relation to the nuclear lamina. For quantitative image analysis, 3D-Immuno-FISH samples were imaged at 1,000× with 2× optical zoom, with a Z step of 0.12 μm between optical slices using an Olympus Fluoview 1,000; *lacO* and BAC foci were scored as associating with the nuclear lamina by overlaying histograms of signal intensity of *lacO*/BAC signal versus LMNB signal. These analyses were verified using the RGB colocalization plug-in in NIH ImageJ (http://rsb.info.nih.gov/ij/).

Cell Cycle Analysis

To synchronize cells, 5 μm aphidicolin was added for 16 hr and then washed out. Cells progressed to mitosis roughly 6–7 hr after removal of aphidicolin, and were then fixed for immunofluorescence analysis. Propidium iodide staining and FACS were used to analyze DNA content. Cell cycle parameters were enumerated using the Modfit modeling software. The complete DamID and ChIPseq data sets can be accessed at http://www.ncbi.nlm.nih.gov/projects/geo/query/acc.cgi?acc=GSE36049.

SUPPLEMENTAL INFORMATION

Supplemental Information includes Extended Experimental Procedures, seven figures, and four tables and can be found with this article online at doi:10.1016/j.cell.2012.04.035.

ACKNOWLEDGMENTS

We acknowledge support from the University of Chicago Functional Genomics Facility for genome-wide expression and DamID analyses. We thank Lázló Kömüves and Allison Bruce at Genentech for assistance with confocal imaging and graphics art, respectively. We are grateful to members of the Singh laboratory for critical input. J.M.Z. was supported by an NIH training grant. I.A.D. acknowledges support by the Cancer Research Institute. H.S. acknowledges support by the Howard Hughes Medical Institute and the Chicago Biomedical Consortium and from NIH GM086213. H.S. and C.J.S. are employees of Genentech Inc.

Received: August 30, 2010
Revised: January 18, 2012
Accepted: April 20, 2012
Published: June 21, 2012

REFERENCES

Adkins, N.L., Hagerman, T.A., and Georgel, P.J. (2006). GAGA protein: a multi-faceted transcription factor. Biochem. Cell Biol. *84*, 559–567.

Ahmed, S., Brickner, D.G., Light, W.H., Cajigas, I., McDonough, M., Froysht-eter, A.B., Volpe, T., and Brickner, J.H. (2010). DNA zip codes control an ancient mechanism for gene targeting to the nuclear periphery. Nat. Cell Biol. *12*, 111–118.

Bailey, T.L.E. (1994). Fitting a mixture model by expectation maximization to discover motifs in biopolymers. Proc. Second Int. Conference on Intelligent Systems for Mol. Biol. *2*, 28–36.

Bertolino, E., Reddy, K., Medina, K.L., Parganas, E., Ihle, J., and Singh, H. (2005). Regulation of interleukin 7-dependent immunoglobulin heavy-chain variable gene rearrangements by transcription factor STAT5. Nat. Immunol. *6*, 836–843.

Bhaskara, S., Knutson, S.K., Jiang, G., Chandrasekharan, M.B., Wilson, A.J., Zheng, S., Yenamandra, A., Locke, K., Yuan, J.L., Bonine-Summers, A.R., et al. (2010). Hdac3 is essential for the maintenance of chromatin structure and genome stability. Cancer Cell *18*, 436–447.

Bhat, K.M., Farkas, G., Karch, F., Gyurkovics, H., Gausz, J., and Schedl, P. (1996). The GAGA factor is required in the early Drosophila embryo not only for transcriptional regulation but also for nuclear division. Development *122*, 1113–1124.

Bolland, D.J., Wood, A.L., Johnston, C.M., Bunting, S.F., Morgan, G., Chakalova, L., Fraser, P.J., and Corcoran, A.E. (2004). Antisense intergenic transcription in V(D)J recombination. Nat. Immunol. *5*, 630–637.

Brown, C.R., and Silver, P.A. (2007). Transcriptional regulation at the nuclear pore complex. Curr. Opin. Genet. Dev. *17*, 100–106.

de Nooijer, S., Wellink, J., Mulder, B., and Bisseling, T. (2009). Non-specific interactions are sufficient to explain the position of heterochromatic chromocenters and nucleoli in interphase nuclei. Nucleic Acids Res. *37*, 3558–3568.

Feng, Y.Q., Seibler, J., Alami, R., Eisen, A., Westerman, K.A., Leboulch, P., Fiering, S., and Bouhassira, E.E. (1999). Site-specific chromosomal integration in mammalian cells: highly efficient CRE recombinase-mediated cassette exchange. J. Mol. Biol. *292*, 779–785.

Finlan, L.E., Sproul, D., Thomson, I., Boyle, S., Kerr, E., Perry, P., Ylstra, B., Chubb, J.R., and Bickmore, W.A. (2008). Recruitment to the nuclear periphery can alter expression of genes in human cells. PLoS Genet. *4*, e1000039.

Galéra, P., Musso, M., Ducy, P., and Karsenty, G. (1994). c-Krox, a transcriptional regulator of type I collagen gene expression, is preferentially expressed in skin. Proc. Natl. Acad. Sci. USA *91*, 9372–9376.

Guelen, L., Pagie, L., Brasset, E., Meuleman, W., Faza, M.B., Talhout, W., Eussen, B.H., de Klein, A., Wessels, L., de Laat, W., and van Steensel, B. (2008). Domain organization of human chromosomes revealed by mapping of nuclear lamina interactions. Nature *453*, 948–951.

He, X., Park, K., and Kappes, D.J. (2010). The role of ThPOK in control of CD4/CD8 lineage commitment. Annu. Rev. Immunol. *28*, 295–320.

Kind, J., and van Steensel, B. (2010). Genome-nuclear lamina interactions and gene regulation. Curr. Opin. Cell Biol. *22*, 320–325.

Kosak, S.T., Skok, J.A., Medina, K.L., Riblet, R., Le Beau, M.M., Fisher, A.G., and Singh, H. (2002). Subnuclear compartmentalization of immunoglobulin loci during lymphocyte development. Science *296*, 158–162.

Kumaran, R.I., and Spector, D.L. (2008). A genetic locus targeted to the nuclear periphery in living cells maintains its transcriptional competence. J. Cell Biol. *180*, 51–65.

Lamond, A.I., and Spector, D.L. (2003). Nuclear speckles: a model for nuclear organelles. Nat. Rev. Mol. Cell Biol. *4*, 605–612.

Li, Y., Cui, Y., Hart, S.N., Klaassen, C.D., and Zhong, X.B. (2009). Dynamic patterns of histone methylation are associated with ontogenic expression of the Cyp3a genes during mouse liver maturation. Mol. Pharmacol. *75*, 1171–1179.

Margalit, A., Brachner, A., Gotzmann, J., Foisner, R., and Gruenbaum, Y. (2007). Barrier-to-autointegration factor—a BAFfling little protein. Trends Cell Biol. *17*, 202–208.

Matharu, N.K., Hussain, T., Sankaranarayanan, R., and Mishra, R.K. (2010). Vertebrate homologue of Drosophila GAGA factor. J. Mol. Biol. *400*, 434–447.

Meister, P., Towbin, B.D., Pike, B.L., Ponti, A., and Gasser, S.M. (2010). The spatial dynamics of tissue-specific promoters during C. elegans development. Genes Dev. *24*, 766–782.

Melnick, A., Carlile, G., Ahmad, K.F., Kiang, C.-L., Corcoran, C., Bardwell, V., Prive, G.G., and Licht, J.D. (2002). Critical residues within the BTB domain of PLZF and Bcl-6 modulate interaction with corepressors. Mol. Cell. Biol. *22*, 1804–1818.

Misteli, T., and Soutoglou, E. (2009). The emerging role of nuclear architecture in DNA repair and genome maintenance. Nat. Rev. Mol. Cell Biol. *10*, 243–254.

Peric-Hupkes, D., Meuleman, W., Pagie, L., Bruggeman, S.W.M., Solovei, I., Brugman, W., Gräf, S., Flicek, P., Kerkhoven, R.M., van Lohuizen, M., et al. (2010). Molecular maps of the reorganization of genome-nuclear lamina interactions during differentiation. Mol. Cell *38*, 603–613.

Pique-Regi, R., Monso-Varona, J., Ortega, A., Seeger, R.C., Triche, T.J., and Asgharzadeh, S. (2008). Sparse representation and Bayesian detection of genome copy number alterations from microarray data. Bioinformatics *24*, 309–318.

Raff, J.W., Kellum, R., and Alberts, B. (1994). The Drosophila GAGA transcription factor is associated with specific regions of heterochromatin throughout the cell cycle. EMBO J. *13*, 5977–5983.

Ragoczy, T., Bender, M.A., Telling, A., Byron, R., and Groudine, M. (2006). The locus control region is required for association of the murine beta-globin locus with engaged transcription factories during erythroid maturation. Genes Dev. *20*, 1447–1457.

Reddy, K.L., Zullo, J.M., Bertolino, E., and Singh, H. (2008). Transcriptional repression mediated by repositioning of genes to the nuclear lamina. Nature *452*, 243–247.

Robinett, C.C., Straight, A., Li, G., Willhelm, C., Sudlow, G., Murray, A., and Belmont, A.S. (1996). In vivo localization of DNA sequences and visualization of large-scale chromatin organization using lac operator/repressor recognition. J. Cell Biol. *135*, 1685–1700.

Schirmer, E.C., and Foisner, R. (2007). Proteins that associate with lamins: many faces, many functions. Exp. Cell Res. *313*, 2167–2179.

Shimi, T., Pfleghaar, K., Kojima, S.-i., Pack, C.-G., Solovei, I., Goldman, A.E., Adam, S.A., Shumaker, D.K., Kinjo, M., Cremer, T., and Goldman, R.D. (2008). The A- and B-type nuclear lamin networks: microdomains involved in chromatin organization and transcription. Genes Dev. *22*, 3409–3421.

Somech, R., Shaklai, S., Geller, O., Amariglio, N., Simon, A.J., Rechavi, G., and Gal-Yam, E.N. (2005). The nuclear envelope protein and transcriptional repressor LAP2beta interacts with HDAC3 at the nuclear periphery, and induces histone H4 deacetylation. J. Cell Sci. *118*, 4017–4025.

Sutherland, H., and Bickmore, W.A. (2009). Transcription factories: gene expression in unions? Nat. Rev. Genet. *10*, 457–466.

Taddei, A., Hediger, F., Neumann, F.R., Bauer, C., and Gasser, S.M. (2004). Separation of silencing from perinuclear anchoring functions in yeast Ku80, Sir4 and Esc1 proteins. EMBO J. *23*, 1301–1312.

Taddei, A., Schober, H., and Gasser, S.M. (2010). The budding yeast nucleus. Cold Spring Harb. Perspect. Biol. *2*, a000612.

Vogel, M.J., Peric-Hupkes, D., and van Steensel, B. (2007). Detection of in vivo protein-DNA interactions using DamID in mammalian cells. Nat. Protoc. *2*, 1467–1478.

Webster, M., Witkin, K.L., and Cohen-Fix, O. (2009). Sizing up the nucleus: nuclear shape, size and nuclear envelope assembly. J. Cell Sci. *122*, 1477–1486.

Wen, B., Wu, H., Shinkai, Y., Irizarry, R.A., and Feinberg, A.P. (2009). Large histone H3 lysine 9 dimethylated chromatin blocks distinguish differentiated from embryonic stem cells. Nat. Genet. *41*, 246–250.

Yang, Q., Riblet, R., and Schildkraut, C.L. (2005). Sites that direct nuclear compartmentalization are near the 5′ end of the mouse immunoglobulin heavy-chain locus. Mol. Cell. Biol. *25*, 6021–6030.

Yokochi, T., Poduch, K., Ryba, T., Lu, J., Hiratani, I., Tachibana, M., Shinkai, Y., and Gilbert, D.M. (2009). G9a selectively represses a class of late-replicating genes at the nuclear periphery. Proc. Natl. Acad. Sci. USA *106*, 19363–19368.

Yu, J., Li, Y., Ishizuka, T., Guenther, M.G., and Lazar, M.A. (2003). A SANT motif in the SMRT co-repressor interprets the histone code and promotes histone deacetylation. EMBO J. *22*, 3403–3410.

Zink, D., Amaral, M.D., Englmann, A., Lang, S., Clarke, L.A., Rudolph, C., Alt, F., Luther, K., Braz, C., Sadoni, N., et al. (2004). Transcription-dependent spatial arrangements of CFTR and adjacent genes in human cell nuclei. J. Cell Biol. *166*, 815–825.